Multi-Vehicle Dynamic Pursuit with Acoustics and Coarse Quantization

Brooks L. Reed[†], **Josh Leighton**[*], **Mei Yi Cheung**[*], **and Franz S. Hover**[*]
[†] MIT/WHOI Joint Program in Oceanographic Engineering
brooksr8@mit.edu
[*] Massachusetts Institute of Technology
Department of Mechanical Engineering
77 Massachusetts Ave, Cambridge MA 02139
{jleight, mc2922, hover}@mit.edu

***Abstract*—Marine robots communicating wirelessly is an increasingly attractive means for observing and monitoring in the ocean, but acoustic communication remains a major impediment to real-time control. In this paper we address through experiments the capability of acoustics to sustain highly dynamic, multi-agent missions, in particular range-only pursuit in a challenging shallow-water environment. Coarse quantization enables fully joint estimation and coordinated control for a pair of vehicles chasing a moving target, entirely through acoustic means. Using 13-bit mini-packets, we achieve a cycle time of 12 seconds and a tracking bandwidth of 0.125rad/s.**

I. Introduction

Marine robots have played an increasing role in ocean operations during recent years, with the proliferation of many commercial platforms, systems and sensors. A major trend is toward tetherless operations, for which each vehicle has to carry its own power source and have a means of wireless communication. Over distances beyond about one hundred meters, underwater communication is almost exclusively accomplished through acoustics, and the wireless nature of this channel lends itself naturally to multiple agents. Acoustic communications bring many challenges, however, such as packet loss, low data rates, and delays; Heidemann *et al.* provide a recent review [1]. These undesirable properties of acoustic communications have limited its use in high-performance, real-time tasks. Typical experiments with acoustic modems address packet loss rates between vehicles [2], [3], distributed navigation [4], and communication of commands [5] or sensor data [6] between vehicles and ships.

If a capability existed, truly dynamic missions of interest would include networked ocean vehicles following a submarine or a marine animal; the latter has been a dream of biologists for decades. Major gaps exist in our understanding of the life cycles of many important marine animals, such as jellyfish [7], sharks [8], [9], tuna [10], lobsters [11], and more. Dynamic pursuit with marine vehicles and appropriate sensors can help give biologists the data they need to fill in these gaps.

A broader and more challenging problem is monitoring and following a quickly-evolving plume or other oceanic process [12], [13], where distributed measurements become critical for assimilation with models and subsequent adaptive sampling [14], [15]. These tasks involve *dynamic feedback control that relies explicitly on acoustic communication*, and fit into the growing field of network-based control [16]. In an effort to lay some groundwork for exploiting advanced algorithms in a real-world ocean application, this paper addresses with experiments an approach for joint estimation and pursuit of a moving target using acoustic communications; see **Figure 1**.

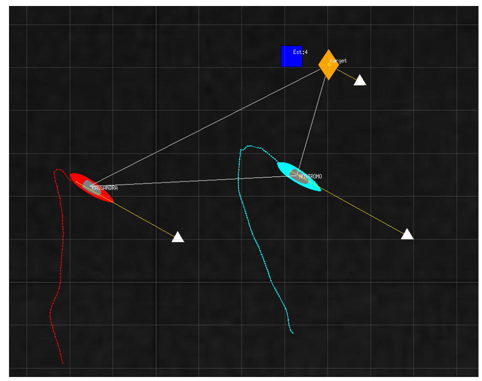

Fig. 1. Screenshot from Team Underwater Localization and Pursuit (TULiP) experiment with acoustic communications. The two vehicles jointly estimate the target location based on range measurements, and move to stay in formation relative to it.

Needless to say, the general pursuit problem has held high interest for decades; it is a canonical mission in space and air, on land, and at sea. Probabilistic pursuit-evasion games have been studied extensively in the robotics literature [17], and pursuer and evader dynamics as well as nonlinear estimation are important factors in these algorithms [18], [19]. However, the effects of communication constraints have not received much attention [20]. These are often addressed indirectly via decentralized approaches that require minimal exchange of information between agents [21]; see [22], [23] for ocean-specific implementations.

There have also been, however, some very recent works that are related to our pursuit scenario. Perhaps most intriguing is tracking a leopard shark in extremely shallow water, using a single autonomous vehicle with a hydrophone array of 2.4m spread [24]. The system was successful but the shark evidently moved only 200m or so in 48 minutes reported. Bean *et al.* (2007) studied range-based leader–follower regulation with MicroModem mini-packets with 1m/s speeds [25], while

Brignone *et al.* (2009) study a similar problem with DSP-Comm modems and two vehicles operating at 0.7 and $3m/s$ [26]. Both works present limited data from proof-of-concept field trials. Soares *et al.* (2013) consider triangle formation-flying where a single follower receives ranging pings from each of two leaders, with leader headings embedded in the pings. The ranges are about fifteen meters, the speeds about $0.5m/s$, and the total loop time is four seconds [27]. In contrast, Cruz *et al.* (2012) consider a complete feedback system—in the sense of two-way communications—for which a stationary controller transmits commands for two mobile followers, who then transmit back their positions [28]. The vehicle speeds are quite slow, in the neighborhood of $10cm/s$, and the cycle time is around twenty seconds. Through analysis, Chen and Pompili (2012) addressed optimization of the special considerations of acoustic communications in coordinated flight of ocean gliders, where currents are especially important [29].

None of these prior works explicitly deal with designing and improving closed-loop frequency response of an integrated multi-vehicle feedback system. This is exactly our objective here. We investigate the use of coarse quantization with 13-bit mini-packets in an effort to minimize cycle time. Further experiments, to appear in [30], bracket the current results between the case of perfect communications ("vehicle with towed array") and lossy but full-resolution packets. Our control and estimation design does not rigorously account for modeling errors, stability margins, the multi-rate nature of acoustic communications, inherent geometric nonlinearities, or the fact that automous marine vehicles are not ideal actuators. On the other hand, our approach clearly demonstrates practical closed-loop performance at half the Nyquist rate, with little evidence of stability breakdown.

We detail the experiment setup in the following section, including descriptions of the vehicles and communication hardware used, the physical environment where the experiment was performed, and the estimation and control strategies and parameters. We then give results from an integrated test, demonstrating the performance achieved.

II. Experimental Setup

Our experiment, **T**eam **U**nderwater **L**ocal**i**zation and **P**ursuit (TULiP), has two mobile agents sharing range information and commands through acoustic links. We make scalar range measurements at each agent, and thus tracking is impossible without their coordination. One agent is designated as the leader that coordinates the measurements and the actions of one or more followers. This arrangement involves lossy channels at both locations in the feedback loop of **Figure 2**. In the general case, a centralized architecture such as this allows integration with remote sensing, large-scale computations (such as data assimilation), and human-in-the-loop decision-making. For our pursuit scenario, a distributed mobile array that utilizes range measurements offers benefits of simpler sensors, more maneuverable vehicles, and increased flexibility compared to systems relying on bearing measurements. However, even when directional or gradient information is available at a single agent, e.g. through a towed array of hydrophones or sensors, exploiting multiple vehicles should give a substantial improvement in the overall mission objectives.

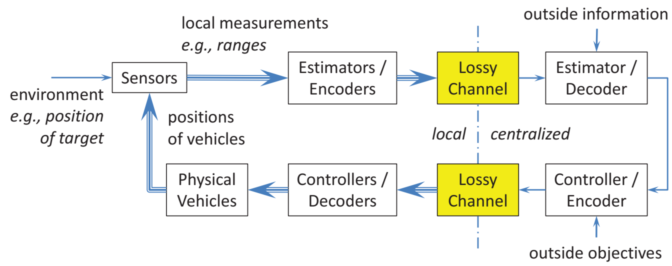

Fig. 2. Block diagram of a generic multi-vehicle feedback system with a centralized estimator and controller, and communication channels in two locations in the loop. Vehicles act as mobile sensors.

The mobile agents attempt to stay close to the target, and in a formation conducive to good sensor performance. The objective of close pursuit as opposed to just tracking (for example, with fixed transponders located far away) has specific benefits. Acoustic sound pressure level drops off with distance, so SNR is higher when vehicles are closer to the target. Additionally, in complex and potentially cluttered environments, line-of-sight is more likely if the pursuit formation is nearby; there is also less chance of a noise source crossing between the target and the pursuers.

The next five subsections detail the arrangement and operation of this complex system.

A. Autonomous Surface Vehicles

We use autonomous kayaks as shown in **Figure 3** for our experiments; they are also described in [31]. Each craft is $1.8m$ long, weighs about $40kg$, and has a rotating thruster near the bow for propulsion and steering. In these tests, the vehicles operate at a nominal speed of $V = 1.5m/s$. The relevant navigation sensors available on each vehicle are a tilt-compensated compass and RTK GPS. We use Novotel GPS antennas, uBlox GPS receivers, and the RTKlib software package [32]. With a fixed base station on shore and communications over wifi, we have observed GPS position variances on the order of $10^{-4}m^2$. Raw compass measurements are passed through a first-order low-pass filter with time constant $1.95s$, and the noise variance on this signal is estimated as $10deg^2$.

The vehicles run MOOS-IvP autonomy software [33] integrated with custom control algorithms and modem interfaces. We rely on the the MOOS heading PID controller, which runs at five Hz, and the MOOS trackline controller, which runs at two Hz. Step response experiments with the kayak under closed-loop heading control indicate a rise time of roughly four seconds, and 30% overshoot; we also note the kayaks are able to turn 180 degrees in approximately three seconds. The MOOS trackline controller is an inner-outer loop that modulates the desired vehicle heading so as to steer it toward a point on the trackline, some lead distance l_d ahead. When the

Fig. 3. The Charles River Basin in Cambridge/Boston, MA, and the autonomous kayak Nostromo. Water depth is 2-12m.

waypoint is closer than the lead distance, the vehicle simply drives towards the waypoint. For longer distances the result for small errors is a proportional map for desired heading: $\phi^d \simeq e_x/l_d$, where e_x is the cross-track error in meters and ϕ^d is in radians.[1] We set $l_d = 15m$ for these experiments.

B. Acoustic Communications

We use the the WHOI Micro-Modem [34], a well-established and commercially available technology for underwater acoustic communication. Modems are towed by the vehicles, suspended at a depth of about 1.5 meters; this gives us realistic shallow-water acoustic performance, but with direct access to GPS and RF wireless connectivity at the surface for conducting controlled tests. Along with messaging, we use the modem for one-way travel-time ranging [35]. The WHOI MicroModem has six different packet types with different lengths and data capacities. In this work, we use the FSK mini-packet, which is regarded as the most robust of the packet types, but contains only thirteen bits of information. The mini-packets take slightly over one second to transmit; we have found communications to be most reliable with four-second slots.

The Charles River Basin has fresh water 2-12m deep, a complex bathymetry, and some hard surfaces on the boundaries (seawalls and bridges); our working space is about 1500m long and 500m wide. Acoustic performance in this environment is different from an open-water deep ocean scenario, where multipath and reverberation are much lower, but the ranges are higher. Operations in the Basin can have highly variable acoustic performance, as shown in **Figure 4**. Our conditions are multipath-limited and travel times are short.

C. TULiP Physical Layout

The two-vehicle pursuit mission encompasses limited communication performance in both the sensing and control channels. In this experiment there is a target to be tracked, "Icarus", and two cooperating agents "Silvana" and "Nostromo". We will denote these three nodes with the symbols $\mathcal{I}$, $\mathcal{S}$, and $\mathcal{N}$, respectively. $\mathcal{N}$ can be thought of as a leader, and $\mathcal{S}$ a follower; our basic approach extends easily to multiple followers. The sensing objective is a simple one: to maintain $\mathcal{S}$ and $\mathcal{N}$ in fixed triangular configuration relative to the estimated location of $\mathcal{I}$, so that measurements will be of high fidelity, *i.e.*, in the sense of a good HDOP [36], and in the sense of a short range. The desired observation triangle has a sixty-degree vertex at $\mathcal{I}$. The ranges to each of $\mathcal{S}$ and $\mathcal{N}$ were $50m$.[2] Maintaining a close pursuit formation keeps ranges near a nominal value with small perturbations, allowing for more precise quantization as discussed in the following section.

However, an unstable situation is encountered if the target crosses the baseline (the line in between the two vehicles acting as a moving LBL network); when this occurs the estimate begins to diverge from the target location. The disadvantage of a small pursuit formation is that it is easier for the target to cross the baseline, bringing up a tradeoff between robustness of a larger formation and accuracy of a smaller formation. Both estimation and control performance must be high for the accuracy of the smaller formation to be realized. We discuss some of these choices in the following sections.

D. Cycle Description, Timing and Quantization

We detail the stages of the control loop. Within a cycle step, $\mathcal{S}$ and $\mathcal{N}$ each receive a measurement of range to $\mathcal{I}$ via the long-baseline (LBL) capability of the Micro-Modems. After a guard period, $\mathcal{S}$ transmits its current location and range data to $\mathcal{N}$ through acoustic communication. $\mathcal{N}$ combines this information with its own location and range information to generate an estimated location of $\mathcal{I}$. $\mathcal{N}$ calculates control actions for itself and for $\mathcal{S}$, and transmits the latter back to $\mathcal{S}$, again through the Micro-Modems and subject to a guard time. The cycle includes three separate transmissions and there are no acknowledgments. The network time protocol is used to synchronize the clocks on each vehicle. We enforce the fixed time slots with a number of timeouts, as indicated in **Figure 5**. In the absence of clock synchronization, we note that precision clocks are becoming increasingly practical for use on underwater vehicles [35].

For feedback control, there is a problem-dependent tradeoff to be made between time-averaged throughput (usually achieved with long coding blocks) and timeliness of the information (shorter messages). Here we present data using 13-bit mini-packets to show one end of the tradeoff curve—minimizing cycle time at the expense of quantization. For the message from $\mathcal{S}$ to $\mathcal{N}$, we used three bits for the range, and five bits each direction for $\mathcal{S}$'s location in a 32×32 discretized workspace; this workspace had ten-meter resolution. For the message from $\mathcal{N}$ back to $\mathcal{S}$, we used five bits in x and y for the desired location in the workspace. This left three bits unused.

[1]The linear form written is based on approximation of the tangent function. For errors less than one meter, the MOOS Trackline controller increases the lead distance proportionally, effectively lowering the gain to limit oscillations.

[2]The ranges are set relative to the distance the target can drive in a time step, so that the target is unlikely to cross the baseline before the control system can react.

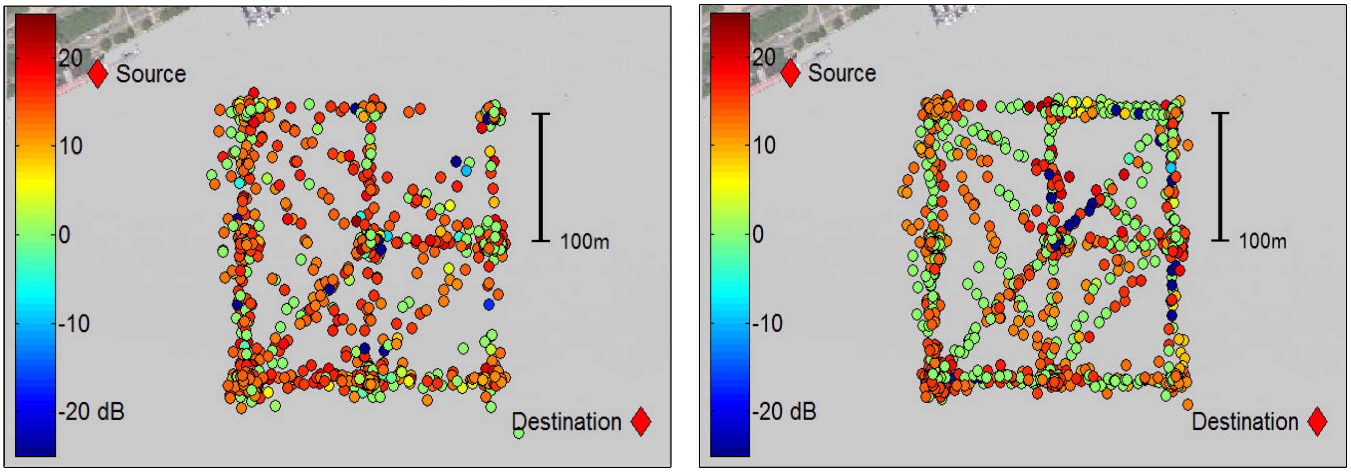

Fig. 4. Micro-Modem performance data in the Charles River Basin, an environment limited by multipath, not power. The left plot shows transmissions from a source to a mobile relay, and the right plot shows transmissions from the relay to a destination. The SNR value indicates sound pressure level relative to ambient noise.

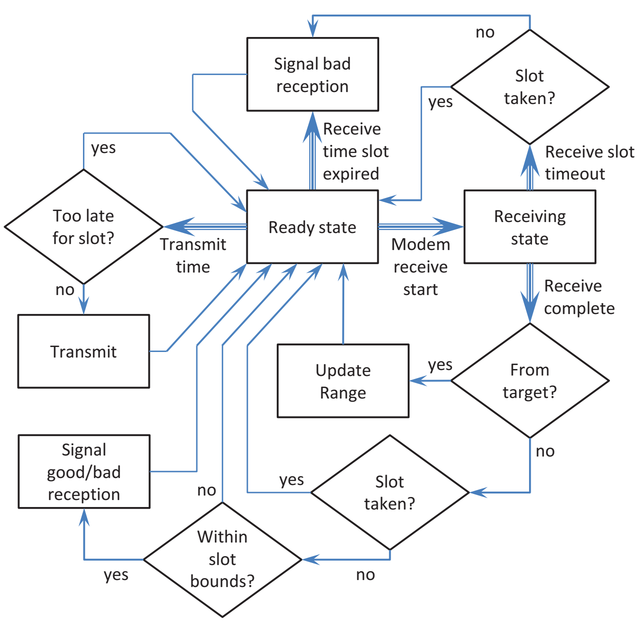

Fig. 5. The internal state machine used on each vehicle in the TULiP mission to maintain consistent timing with respect to predefined transmission and reception slots. Thick arrows distinguish acoustic events that initiate state changes or other actions from normal logic flow. Special operations are indicated to handle detection of erroneous multipath receptions, which frequently occur in this environment. For example, a good reception for a time slot T_i will follow the "Receive complete" path (bottom) to a good signal. A trailing multipath reception will return to the receiving state, but the end of time slot T_i will arrive before the end of the packet. In the top right, slot T_i is already taken by the good reception, so we return to the ready state with no action taken.

The total cycle time we achieved with the mini-packets was twelve seconds.

The range data were logarithmically quantized relative to a desired range of $50m$, with seven bin edges located at $[19.2\ 32.5\ 42.5\ 50\ 57.5\ 67.5\ 80.8]m$, and the three-bit messages decoded as $[11.5\ 26.8\ 38.2\ 46.8\ 53.2\ 61.8\ 73.2\ 88.5]m$. This correlates with the density $\rho = 0.75$ [37]. Note that with quantization, there is a tradeoff between range and precision. With this choice, any range larger than $80.8m$ is decoded as the furthest range bin, so when ranges are very large, estimation suffers. Increasing this outer range would come at the expense of resolution of smaller bins near the $50m$ middle range; it is the job of the control system to keep the vehicles in the desired formation so that higher-resolution middle bins are used.

We have also considered two different cases in other experiments. Using full-resolution, 32-byte FSK0 packets instead of mini-packets required a 23-second cycle time, while the case of perfect wifi communications required a 4-second cycle time. Additionally, as we were submitting this paper we became aware of several modifications in the operation of the MicroModems that likely will allow for faster cycle times. Thus, the current results should not be seen as limiting cases of MicroModem performance, although they are still highly representative of what one will encounter in applications.

E. Settings and User Choices

The tracking system contains a nonlinear sigma-point filter (SPF) [38], well-suited for this type of application.[3] The nonholonomic target is assumed to be moving at constant speed in the plane of $1.55m/s$, with stochastic low-pass, zero-mean turning rate with variance $Q = 0.05(rad/s)^2$. These values are set to be consistent with the motion of the small motorboat that was $\mathcal{T}$. The observation vector contains the two

[3]Other nonlinear, range-only filters, such as particle filters, could also be used [39].

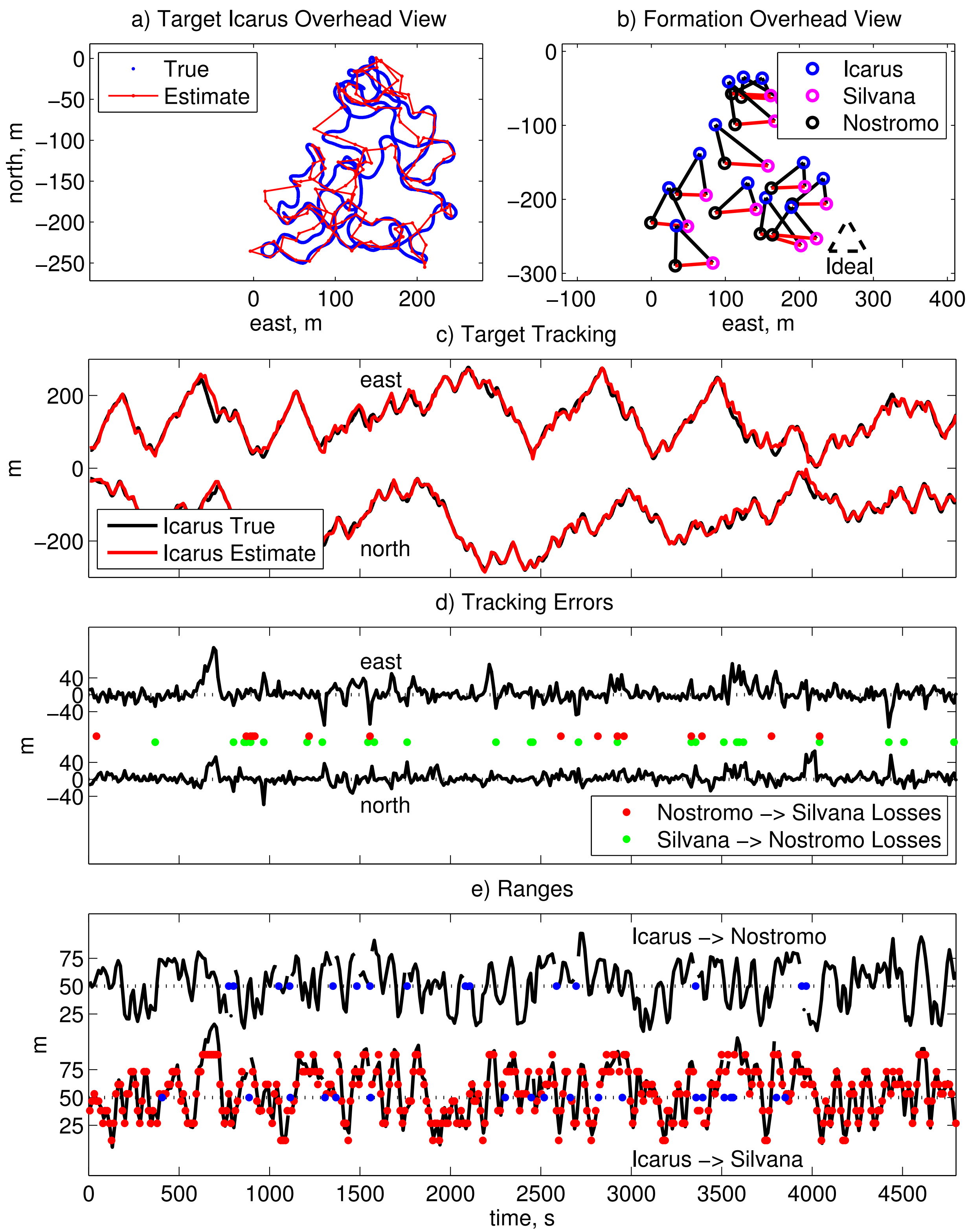

Fig. 6. Results (4800 seconds, 400 cycles). a) Overview of the true and estimated trajectories of the target Icarus (the segment from 1000-3000 seconds is shown for clarity). b) Sensing formation every 15 time steps (the segment from 1000-3000 seconds is shown for clarity). c) Actual (GPS) and estimated trajectory of the target Icarus. d) Estimation error of Icarus' location. The RMS radius of estimation errors was $12.7m$. Data packet losses are also shown; the loss rates were: $\mathcal{N} \rightarrow \mathcal{S} = 3.8\%$, $\mathcal{S} \rightarrow \mathcal{N} = 6.5\%$. e) Range measurements from Icarus to each vehicle, and losses. Range loss rates were: $\mathcal{I} \rightarrow \mathcal{N} = 3.8\%$, $\mathcal{I} \rightarrow \mathcal{S} = 4.8\%$. Quantized measurements sent from Silvana to Nostromo are shown in red on top of the true measured ranges.

noisy ranges, with variances $R_S = 9m^2$ and $R_N = 0.25m^2$ for range measurements to Silvana and Nostromo, respectively. The sensor noise for leader range measurements ($\mathcal{J}$ to $\mathcal{N}$) was chosen based on prior characterizations of the WHOI Micro-Modem ranging capability [34], [40] and our own observed LBL performance. The sensor noise for the follower range measurement ($\mathcal{J}$ to $\mathcal{S}$) was set to a higher value to account for the effects of quantization during communication of the measurement from $\mathcal{S}$ to the filter running on $\mathcal{N}$.

When a measurement is not available (either due to a missed LBL range, or a dropped measurement packet from $\mathcal{S}$ to $\mathcal{N}$), we take the standard approach of setting the noise of the lost measurement to infinity [41]. When a control command from $\mathcal{N}$ to $\mathcal{S}$ is dropped, the previously-received command for $\mathcal{S}$ remains the desired waypoint; this can be viewed as a zero-output decoder on the controller communication channel. This approach is chosen to ensure safe operation in the case of many missed packets—it is less likely for the system to have stability problems (*e.g.* target crossing the baseline of the LBL formation) with this approach compared to approaches where the vehicles continue to drive (in the wrong direction). Three bits are left unused in the command packet which could encode contingency plans in the case of future dropped command packets.

III. Experimental Results

The experiment we report was conducted on 8 July 2013, a day with light winds.[4]

Figure 6 gives results from an 80-minute test (400 cycles). The target $\mathcal{J}$ moved in a largely random trajectory, as shown in the birds-eye view in the upper left of the plot (Subplot **a**) and the time traces in Subplot **c**. The upper right (Subplot **b**) shows the sensing formation every fifteen time steps; we see that while the ideal triangle configuration was rarely achieved, the target did not cross the baseline (the red straight line between the two nodes acting as a moving LBL network), nor did the geometry ever stay poor for a sustained period. The tracking and pursuit system did not lose the target.

The measured ranges are reported in the lower subplot, including quantization of raw values sent to $\mathcal{N}$ from $\mathcal{S}$ in the subsequent measurement packet. Range losses are low, as the MicroModem ranging ping is fairly robust; see figure captions for loss statistics. Subplot **d** shows the north and east tracking error over time, along with dropped communication packets. Most of the larger errors occur following packet losses, especially clusters of back-to-back losses of measurements and control commands. However, some large spikes are not near packet losses—errors can also occur due to poor sensing geometry and quantization, which are often related to each other. For example, near 700 seconds the range from $\mathcal{J}$ to $\mathcal{S}$ is very large, corresponding to a skewed formation as well as a large quantization error (the difference between the black trace and the red dots in Subplot **e**).

[4]This data will soon be publicly available at http://web.mit.edu/hovergroup/resources.html .

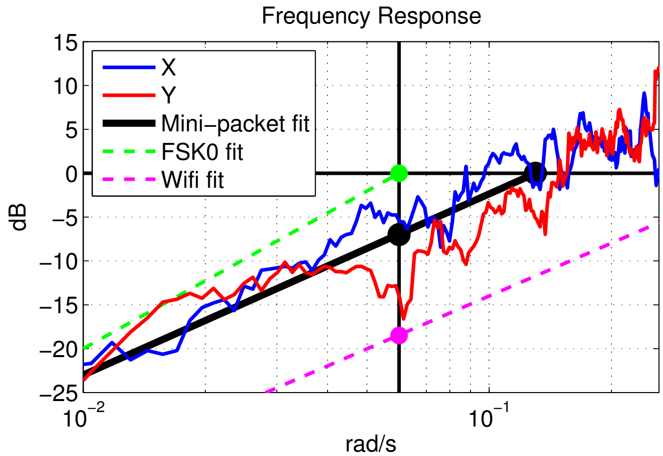

Fig. 7. Empirical FFT-based transfer function for estimator error divided by target motion when tracking using mini-packets (MP). The thick black line shows an approximate linear fit for low-frequency attenuation. For comparison, the approximate fits from tests reported in [30] are also shown; dashed green for full-sized FSK0 packets and dashed magenta for wifi ("single vehicle with array") communications. Dots show the approximate attenuation at $0.06 rad/s$ (the bandwidth of the FSK0 test), and the approximate bandwidth for the mini-packet test.

Recalling our broad objective to achieve dynamic control through mobile acoustic networks, it is revealing to ask what is the effective closed-loop estimation bandwidth achieved. A direct FFT-based empirical transfer function for the estimation error divided by target motion is shown in **Figure 7**; spectra have been smoothed with a 5-point centered moving average. The break frequency for tracking the motion of $\mathcal{J}$ is approximately $0.125 rad/s$, about half the Nyquist rate for the twelve-second cycle. For comparison, we also show the approximate fits from results studying the case of perfect wifi communications ("vehicle with towed array") and lossy but full-resolution FSK0 packets. The FSK0 packet test has a break frequency of approximately $0.06 rad/s$, slightly less than half the Nyquist rate for the twenty-three-second cycle required with this packet type. The wifi test has a break frequency of approximately $0.5 rad/s$, over half the Nyquist rate for this cycle time of four seconds. We can also compare the attenuation of tracking error for each configuration at $0.06 rad/s$. FSK0 has zero attenuation, wifi has 19 dB attenuation, and the mini-packet configuration has 7 dB attenuation.

On top of longer cycle times, the mini-packet and FSK0 cases are affected by communication packet losses, and the mini-packets also by quantization, so the degradation in performance compared to wifi is expected. We note that the surface vehicles we use (and underwater vehicles without arrays) are highly maneuverable; a true "single vehicle with array" configuration would be subject to much more stringent maneuverability constraints and could not pursue the target as closely without risking the target crossing the baseline. For close pursuit, we can view the wifi case as a lower bound on performance achievable with realistic communications. The FSK0 and mini-packet results suggest that if tracking bandwidth is desired, it is advantageous to reduce the cycle times as much as possible, even at the expense of extreme quantization.

IV. Conclusion

Our TULiP experiment has achieved aggressive target pursuit in the underwater environment. As opposed to a traditional control and estimation design scenario, the mission here is accomplished through a highly integrated vehicle system performing full joint estimation and coordination through lossy acoustic communications underwater.

More broadly, this pursuit mission addresses many of the fundamental challenges in dynamic ocean observation with autonomous agents. The central elements in network-based control of quantization, delay, update rate, and packet loss all strongly affect the level of performance achieved, and together provide the key design variables. Three-dimensional tracking over larger areas with more pursuers brings up a new set of questions as well. Especially in larger observation networks, specification of physical configurations, scheduling, routing, and multi-rate control design will undoubtedly join the mix, making underwater pursuit a rich problem for future work.

Acknowledgments

Work is supported by the Office of Naval Research, Grant N00014-09-1-0700, the National Science Foundation, Contract CNS-1212597, and the Finmeccanica Career Development Professorship. We thank Toby Schneider and Mike Benjamin at MIT, and Keenan Ball and Sandipa Singh at WHOI, for their terrific help on technical items. We also acknowledge MIT Sailing Master Fran Charles.

References

[1] J. Heidemann, M. Stojanovic, and M. Zorzi, “Underwater sensor networks: applications, advances and challenges,” *Philosophical Transactions of the Royal Society A: Mathematical, Physical and Engineering Sciences*, vol. 370, no. 1958, pp. 158–175, 2012.

[2] A. Caiti, V. Calabro, G. Dini, A. Duca, and A. Munafo, “AUVs as mobile nodes in acoustic communication networks: Field experience at the UAN10 experiments,” in *Proc. MTS/IEEE OCEANS*, 2011.

[3] J. Canning, M. Anderson, D. Edwards, M. O’Rourke, T. Bean, J. Pentzer, and D. Odell, “A low bandwidth acoustic communication strategy for supporting collaborative behaviors in a fleet of autonomous underwater vehicles,” *US Navy J. Underwater Acoustics*, 2009.

[4] A. Bahr, J. Leonard, and M. Fallon, “Cooperative localization for autonomous underwater vehicles,” *International J. Robotics Research*, vol. 28, no. 6, p. 714, 2009.

[5] T. Schneider and H. Schmidt, “Unified command and control for heterogeneous marine sensing networks,” *Journal of Field Robotics*, vol. 27, no. 6, pp. 876–889, 2010.

[6] C. Murphy and H. Singh, “Wavelet compression with set partitioning for low bandwidth telemetry from AUVs,” in *Proc. of the Fifth ACM International Workshop on UnderWater Networks*. ACM, 2010, p. 1.

[7] J. Rife and S. Rock, “Design and validation of a robotic control law for observation of deep-ocean jellyfish,” *IEEE Trans. Robotics*, vol. 22, no. 2, pp. 282 –291, april 2006.

[8] G. Skomal and G. Benz, “Ultrasonic tracking of greenland sharks, somniosus microcephalus, under arctic ice,” *Marine Biology*, vol. 145, no. 3, pp. 489–498, 2004.

[9] F. Voegeli, M. Smale, D. Webber, Y. Andrade, and R. O’Dor, “Ultrasonic telemetry, tracking and automated monitoring technology for sharks,” *Environmental Biology of Fishes*, vol. 60, no. 1, pp. 267–282, 2001.

[10] M. Lutcavage, R. Brill, G. Skomal, B. Chase, J. Goldstein, and J. Tutein, “Tracking adult north atlantic bluefin tuna (thunnus thynnus) in the northwestern atlantic using ultrasonic telemetry,” *Marine Biology*, vol. 137, no. 2, pp. 347–358, 2000.

[11] I. Vázquez-Rowe, D. Iribarren, M. T. Moreira, and G. Feijoo, “Combined application of life cycle assessment and data envelopment analysis as a methodological approach for the assessment of fisheries,” *The International Journal of Life Cycle Assessment*, vol. 15, no. 3, pp. 272–283, 2010.

[12] R. Camilli, C. Reddy, D. Yoerger, B. Van Mooy, M. Jakuba, J. Kinsey, C. McIntyre, S. Sylva, and J. Maloney, “Tracking hydrocarbon plume transport and biodegradation at Deepwater Horizon,” *Science*, vol. 330, no. 6001, p. 201, 2010.

[13] J. Farrell, S. Pang, W. Li, and R. Arrieta, “Chemical plume tracing experimental results with a REMUS AUV,” in *Proc. MTS/IEEE OCEANS*, vol. 2. IEEE, 2003, pp. 962–968.

[14] E. Fiorelli, N. E. Leonard, P. Bhatta, D. A. Paley, R. Bachmayer, and D. M. Fratantoni, “Multi-AUV control and adaptive sampling in Monterey Bay,” *IEEE J. Oceanic Engineering*, vol. 31, pp. 935 –948, 2006.

[15] N. Leonard, D. Paley, F. Lekien, R. Sepulchre, D. Fratantoni, and R. Davis, “Collective motion, sensor networks, and ocean sampling,” *Proc. IEEE*, vol. 95, no. 1, pp. 48 –74, 2007.

[16] J. Baillieul and P. Antsaklis, “Control and communication challenges in networked real-time systems,” *Proc. of the IEEE*, vol. 95, no. 1, pp. 9–28, 2007.

[17] R. Vidal, O. Shakernia, H. Kim, D. Shim, and S. Sastry, “Probabilistic pursuit-evasion games: theory, implementation, and experimental evaluation,” *IEEE Trans. Robotics and Automation*, vol. 18, no. 5, pp. 662 – 669, oct 2002.

[18] E. Liao, G. Hollinger, J. Djugash, and S. Singh, “Preliminary results in tracking mobile targets using range sensors from multiple robots,” *Distributed Autonomous Robotic Systems 7*, pp. 125–134, 2006.

[19] K. Zhou and S. Roumeliotis, “Optimal motion strategies for range-only constrained multisensor target tracking,” *IEEE Trans. Robotics*, vol. 24, no. 5, pp. 1168–1185, 2008.

[20] Y. Mostofi, T. Chung, R. Murray, and J. Burdick, “Communication and sensing trade-offs in decentralized mobile sensor networks: a cross-layer design approach,” in *Proc. 4th International Symposium on Information Processing in Sensor Networks*. IEEE Press, 2005, p. 16.

[21] T. Chung, J. Burdick, and R. Murray, “A decentralized motion coordination strategy for dynamic target tracking,” in *Proc. IEEE International Conference on Robotics and Automation*, 2006, pp. 2416 –2422.

[22] A. Gadre, D. Maczka, D. Spinello, B. McCarter, D. Stilwell, W. Neu, M. Roan, and J. Hennage, “Cooperative localization of an acoustic source using towed hydrophone arrays,” in *Proc. IEEE/OES Autonomous Underwater Vehicles*, oct. 2008, pp. 1 –8.

[23] D. Eickstedt, M. Benjamin, H. Schmidt, and J. Leonard, “Adaptive tracking of underwater targets with autonomous sensor networks,” *US Navy J. Underwater Acoustics*, vol. 56, pp. 465–495, 2006.

[24] C. M. Clark, C. Forney, E. Manii, D. Shinzaki, C. Gage, M. Farris, C. G. Lowe, and M. Moline, “Tracking and following a tagged leopard shark with an autonomous underwater vehicle,” *Journal of Field Robotics*, vol. 30 (3), pp. 309–322, 2013.

[25] T. Bean, J. Canning, G. Beidler, M. ORourke, and D. Edwards, “Designing and implementing collaborative behaviors for autonomous underwater vehicles,” in *Proc. International Symposium on Unmanned Untethered SubmersibleTechnology*, 2007.

[26] L. Brignone, J. Alves, and J. Opderbecke, “GREX sea trials: first experiences in multiple underwater vehicle coordination based on acoustic communication,” in *Proc. MTS/IEEE OCEANS*, 2009.

[27] J. Soares, A. Aguiar, A. Pascoal, and A. Martinoli, “Joint asv/auv range-based formation control: Theory and experimental results,” in *Proc. International Conf. Robotics and Automation (ICRA)*, 2013.

[28] N. A. Cruz, B. M. Ferreira, A. C. Matos, C. Petrioli, R. Petroccia, and D. Spaccini, “Implementation of an underwater acoustic network using multiple heterogeneous vehicles,” in *Proc. MTS/IEEE Oceans*. IEEE, 2012, pp. 1–10.

[29] B. Chen and D. Pompili, “Team formation and steering algorithms for underwater gliders using acoustic communications,” *Computer Communications*, vol. 35, no. 9, pp. 1017–1028, 2012.

[30] B. Reed, J. Leighton, M. Stojanovic, and F. Hover, “Multi-vehicle dynamic pursuit using underwater acoustics,” in *International Symposium on Robotics Research (ISRR), submitted.*, 2013.

[31] E. Gilbertson, B. Reed, J. Leighton, M. Cheung, and F. Hover, "Experiments in dynamic control of autonomous marine vehicles using acoustic modems," in *Proc. IEEE International Conf. on Robotics and Automation*, 2013.
[32] T. Takasu and A. Yasuda, "Development of the low-cost RTK-GPS receiver with an open source program package RTKLIB," in *International Symposium on GPS/GNSS, International Convention Center Jeju, Korea*, 2009.
[33] M. Benjamin, J. Leonard, H. Schmidt, and P. Newman, "An overview of MOOS-IvP and a brief users guide to the IvP helm autonomy software," *Massachusetts Institute of Technology, MIT CSAIL, Tech. Rep. TR-2009-28-07*, 2009.
[34] L. Freitag, M. Grund, S. Singh, J. Partan, P. Koski, and K. Ball, "The WHOI micro-modem: an acoustic communications and navigation system for multiple platforms," in *Proc. MTS/IEEE OCEANS*, 2005.
[35] R. M. Eustice, H. Singh, and L. L. Whitcomb, "Synchronous-clock one-way-travel-time acoustic navigation for underwater vehicles," *J. Field Robotics, Special Issue on State of the Art in Maritime Autonomous Surface and Underwater Vehicles*, vol. 28, no. 1, pp. 121–136, 2011.
[36] B. Bingham, "Predicting the navigation performance of underwater vehicles," in *Proc. IEEE/RSJ Intelligent Robots and Systems, 2009*, 2009.
[37] M. Fu and L. Xie, "The sector bound approach to quantized feedback control," *IEEE Trans. Automatic Control*, vol. 50, no. 11, pp. 1698 – 1711, nov. 2005.
[38] S. Julier and J. Uhlmann, "New extension of the Kalman filter to nonlinear systems," in *AeroSense'97*. International Society for Optics and Photonics, 1997, pp. 182–193.
[39] F. Dellaert, D. Fox, W. Burgard, and S. Thrun, "Monte carlo localization for mobile robots," in *Robotics and Automation, 1999. Proceedings. 1999 IEEE International Conference on*, vol. 2. IEEE, 1999, pp. 1322–1328.
[40] J. Curcio, J. Leonard, J. Vaganay, A. Patrikalakis, A. Bahr, D. Battle, H. Schmidt, and M. Grund, "Experiments in moving baseline navigation using autonomous surface craft," in *Proc. MTS/IEEE OCEANS*, 2005.
[41] B. Sinopoli, L. Schenato, M. Franceschetti, K. Poolla, M. Jordan, and S. Sastry, "Kalman filtering with intermittent observations," *IEEE Trans. Automatic Control*, vol. 49, no. 9, pp. 1453–1464, 2004.